Published in final edited form as:
Dev Biol. 2011 March 1; 351(1): 70–81. doi:10.1016/j.ydbio.2010.12.022.

Synovial joint formation requires local *Ext1* expression and heparan sulfate production in developing mouse embryo limbs and spine

Christina Mundy[a], **Tadashi Yasuda**[a], **Takashi Kinumatsu**[a], **Yu Yamaguchi**[b], **Masahiro Iwamoto**[a], **Motomi Enomoto-Iwamoto**[a], **Eiki Koyama**[a], and **Maurizio Pacifici**[a,*]

[a]Department of Orthopaedic Surgery, College of Medicine, Thomas Jefferson University, Philadelphia, PA 19107, USA

[b]Sanford Children's Health Research Center, Sanford-Burnham Medical Research Institute, La Jolla, CA 92037, USA

Abstract

Heparan sulfate proteoglycans (HSPGs) regulate a number of major developmental processes, but their roles in synovial joint formation remain unknown. Here we created conditional mouse embryo mutants lacking *Ext1* in developing joints by mating *Ext1*$^{f/f}$ and *Gdf5-Cre* mice. *Ext1* encodes a subunit of the Ext1/Ext2 Golgi-associated protein complex responsible for heparan sulfate (HS) synthesis. The proximal limb joints did form in the *Gdf5-Cre;Ext1*$^{f/f}$ mutants, but contained an uneven articulating superficial zone that expressed very low *lubricin* levels. The underlying cartilaginous epiphysis was deranged as well and displayed random patterns of cell proliferation and *matrillin-1* and *collagen IIA* expression, indicative of an aberrant phenotypic definition of the epiphysis itself. Digit joints were even more affected, lacked a distinct mesenchymal interzone and were often fused likely as a result of local abnormal BMP and hedgehog activity and signaling. Interestingly, overall growth and lengthening of long bones were also delayed in the mutants. To test whether Ext1 function is needed for joint formation at other sites, we examined the spine. Indeed, entire intervertebral discs, normally composed by nucleus pulposus surrounded by the annulus fibrosus, were often missing in *Gdf5-Cre;Ext1*$^{f/f}$ mice. When disc remnants were present, they displayed aberrant organization and defective joint marker expression. Similar intervertebral joint defects and fusions occurred in *Col2-Cre;β-catenin*$^{f/f}$ mutants. The study provides novel evidence that local *Ext1* expression and HS production are needed to maintain the phenotype and function of joint-forming cells and coordinate local signaling by BMP, hedgehog and Wnt/β-catenin pathways. The data indicate also that defects in joint formation reverberate on, and delay, overall long bone growth.

*Corresponding author: Maurizio Pacifici, Department of Orthopaedic Surgery, Thomas Jefferson University College of Medicine, 1015 Walnut Street, 501 Curtis Bldg., Philadelphia, PA 19107, Phone (215) 955 7352, Fax (215) 955 9159, maurizio.pacifici@jefferson.edu.

Keywords

Ext1; heparan sulfate; limb synovial joint formation; intervertebral joints; spine; mouse skeletogenesis; lubricin

Introduction

Heparan sulfate proteoglycans (HSPGs) are cell surface and extracellular matrix-associated macromolecules that regulate and modulate a number of major developmental processes (Hacker et al., 2005; Lin, 2004). They consist of a core protein to which one or several heparan sulfate (HS) chains are covalently attached at specific serine residues. The chains are composed of repeating D-glucuronic acid (GlcA) and N-acetyl-D-glucosamine (GlcNAc) residues that are assembled into linear polysaccharides in the Golgi complex by the concerted action of Ext1/Ext2 glycosyltransferase co-polymerase complexes (Esko and Selleck, 2002). During assembly, the nascent chains undergo extensive and physiologically relevant modifications that include N-deacetylation of GlcNAc residues followed by N-sulfation, epimerization of GlcA to iduronic acid (IdoA), and O-sulfation at C2 and C6 of GlcA and IdoA. These complex and systematic reactions are carried out by families of Golgi-resident modifying enzymes, and result in the creation of patterns of specific negatively-charged sulfated segments of modified sugars within the chains of HSPGs expressed in different tissues and organs (Esko and Selleck, 2002). Thus endowed, the HSPGs can influence cell determination, differentiation, shape and migration by regulating processes such as cell-matrix interactions, matrix assembly and organization, and cell-growth factors interactions (Bernfield et al., 1999; Hacker et al., 2005). The latter are of particular relevance since signaling and growth factors critical for skeletogenesis, including bone morphogenetic, hedgehog and Wnt family members, are in fact HS-binding and HS-dependent factors. For example, we and other groups found that Indian hedgehog (Ihh) diffusion, distribution and action in the growth plate of developing skeletal elements and in chondrocytes depend on, and are regulated by, HSPGs (Koyama et al., 2007b; Koziel et al., 2004; Shimo et al., 2004). In addition, gene ablation studies showed that HSPG family members perlecan and glypican-3 have very important roles in long bone development and growth plate function (Arikawa-Hirasawa et al., 1999; Viviano et al., 2005). These and many other studies have provided compelling evidence for the importance of HSPGs in various developmental processes and insights into their mode of action (Bishop et al., 2007), but much remains to be learned about their exact roles in those and other processes, including formation and morphogenesis of synovial joints during limb and axial skeletogenesis.

In the embryonic limb, joint formation initiates with the emergence of the so-called interzone at each prescribed joint site (Archer et al., 2003; Pacifici et al., 2005). The interzone is composed of flat and tightly-packed mesenchymal cells that initially define and delineate the anatomical boundary between adjacent cartilaginous anlagen such as that between femur and tibia or metacarpal and first phalangeal elements (Andersen, 1961; Holder, 1977; Mitrovic, 1978). Original micro-dissection and transplantation studies showed that the interzone is actually needed for joint formation since its removal led to joint ablation and fusion (Holder, 1977). However, it had remained unclear whether the interzone represents a transient but necessary physical barrier for joint site definition and/or whether its cells directly contribute to joint tissue formation. To address this fundamental riddle, we previously carried out genetic cell tracing and tracking experiments using compound transgenic mice. We mated Rosa R26R reporter (*LacZ*) mice with mice producing Cre-recombinase under the control of regulatory sequences from the growth and differentiation factor-5 (*Gdf5*) gene that is normally expressed in nascent limb joint interzone cells

(Rountree et al., 2004). We monitored the fate and roles of *LacZ*-positive interzone cells over time and found that the cells were not at all transient, but in fact gave rise to most if not all joint tissues including articular cartilage layers, intrajoint ligaments and synovial lining (Koyama et al., 2007a; Koyama et al., 2008). The data demonstrated that the interzone mesenchymal cells constitute a specialized and unique cohort of progenitor cells programmed and determined for joint formation. Recent studies have provided further evidence that interzone function and joint formation require mechanical stimulation from the developing musculature (Kahn et al., 2009; Pitsillides, 2006), pointing to interesting interrelationships and interdependencies between the two major limb musculoskeletal systems.

An intriguing and critical aspect of joint formation is that the interzone cells have unique cytological characteristics in terms of an elongated cell shape, tight cell-cell interactions and specific cell-matrix component interactions that could all be potentially influenced by HS-PGs (Bernfield et al., 1999; Hacker et al., 2005). In addition, functioning and developmental behavior of the cells strictly depend on signaling and growth factors molecules that are HS-binding. For instance, *Noggin* ablation in mouse embryos leads to complete limb joint fusion (Brunet et al., 1998) and excessive BMP levels and signaling cause joint fusion as well (Merino et al., 1999). Thus the present study was conducted to tackle the key question as to whether HSPGs are in fact critical for joint formation. We used a loss-of-function approach and created conditional mouse mutants lacking *Ext1* in developing joints and thus producing little if any local HS because of the absence of an essential component of the Golgi-associated Ext1/Ext2 co-polymerase complex.

Materials and Methods

Mouse lines, mating and genotyping

Gdf-5-Cre transgenic mice were described previously (Rountree et al., 2004) and line B was used in the present study. Mice were mated with Rosa R26R Cre-inducible *LacZ* (β-galactosidase) mice in which the reporter β-galactosidase gene is silent and becomes irreversibly expressed after Cre-recombinase removal of a floxed silencer within its constitutive promoter reporter mice (Soriano, 1999). Creation of loxP-modified *Ext1* allele and establishment of the *Ext1* floxed mouse line were described previously (Inatani et al., 2003). Mice conditionally deficient in *β-catenin* were created by mating *β-catenin* floxed mice (*β-catenin*$^{fl/fl}$) possessing loxP sites in introns 1 and 6 of the β-catenin gene (6.129-Ctnnb1tmKem/KnwJ line purchased from the Jackson Laboratory) with *Col2a1-Cre* mice (Ovchinnikov et al., 2000) mice. Pregnant mice and postnatal mice were sacrificed by IACUC approved methods. Genotyping was carried out with DNA isolated from tail clips. Staining for β-galactosidase on whole embryos or tissue sections was accomplished by standard protocols (Lobe et al., 1999).

In situ hybridization and proliferation analysis

In situ hybridization was carried out as described (Koyama et al., 1999). Limbs and spine fixed with 4% paraformaldehyde overnight were embedded in paraffin and sectioned. Serial 5 μm-thick sections from wild type and mutants mounted on the same slide were pretreated with 10 μg/ml proteinase K (Sigma, St. Louis, MO) in 50 mM Tris-HCl, 5 mM EDTA pH 7.5 for 1 min at room temperature, immediately post-fixed in 4% paraformaldehyde buffer for 10 min, and then washed twice in 1X PBS containing 2 mg/ml glycine for 10 min/wash. Sections were treated for 15 min with a freshly prepared solution of 0.25% acetic anhydride in triethanolamine buffer and were hybridized with antisense or sense ^{35}S-labeled riboprobes (approximately 1×10^6 DPM/section) at 50°C for 16 h. cDNA clones used as templates included: a 392 bp mouse *Wnt9a* (547-940; NM_139298); a 550 bp mouse *Gfd5*

(1321-1871; NM_008109); a full length mouse *Erg* (AK142379.1); a 2,605 bp mouse *lubricin* (41-2646; AB034730); a 121bp mouse *collagen IIA* (284-404, NM_008109); a 356bp mouse *collagen IIB* (2409-2764, NM_008109); a 254bp mouse histone 4C (*H4C*) (546-799; AY158963); a 515bp mouse *collagen X* (1302-1816; NM _009925); and a 411bp mouse *Ext1* (256-666, U78539). cDNA clones for *Ihh*, *Gli3* and *Patched1* were described previously (Shibukawa et al., 2007). After hybridization, slides were washed three times with 2X SSC containing 50% formamide at 50°C for 20 min/wash, treated with 20 μg/ml RNase A for 30 min at 37°C, and washed three times with 0.1X SSC at 50°C for 10 min/wash. Sections were dehydrated by immersion in 70, 90, and 100% ethanol for 5 min/step, coated with Kodak NTB-3 emulsion diluted 1:1 with water, and exposed for 10 to 14 days. Slides were developed with Kodak D-19 at 20°C for 3 min, stained with hematoxylin and eosin. Bright and dark-field images of in situ hybridization were taken with a SPOT insight camera (Diagnostic Instruments, Inc.) operated with SPOT 4.0 software, and dark field images were pseudo-colored using Adobe Photoshop software. No further processing of images was performed apart from assembling montages in Photoshop (version 8, Adobe). The *ImageJ* program was used to determine proliferation index in wild type and mutant specimens using the Plugins task bar. Five areas (approximately 100 cells/square) were randomly chosen in different slides, and average numbers of *H4C*-positive cells were calculated blindly and used for statistical analysis by Student t-test to determine significance.

Immunohistochemistry and histochemistry

Immunostaining for HS was carried out with paraffin sections (David et al., 1992) that were first de-paraffinized and then treated with 5 mg/ml testicular hyaluronidase in 5% normal goat serum (NGS) for 1 hr at 37°C to concurrently de-mask the tissue and block non-specific binding. To generate the HS antigen, sections were treated with heparinase III (Sigma) at 5U/ml for 2 hrs at 37°C. Sections were incubated with anti-HS monoclonal antibody 3G10 (Seikagaku) at 1:200 dilution in 3% NGS in PBS for 3 hrs at room temperature. Following rinsing, sections were then incubated with biotinylated anti-mouse IgGs (Vector) at 1:150 dilution in 3% NGS for 30 min at room temperature. Sections were washed with 3% NGS and incubated with Cy3-streptavidin (Zymed) (1:35) in 3% NGS for 30 min at room temperature under dark conditions. Fluorescence images were captured with an inverted Eclipse TE2000-U Nikon microscope using Image-Pro Plus 5.0 software (Media Cybernetics, Inc.)

Immunostaining for phospho-Smad1/5/8 was carried out with the above procedure and the following modification. Following removal of paraffin, sections were subjected to antigen retrieval (Namimatsu et al., 2005) and then incubated with a 1:250 dilution of pSmad1/5/8 antibodies (Cell Signaling) for 3 hrs at room temperature. After rinsing, bound antibodies were localized by incubation with a 1:500 dilution of rhodamine-conjugated goat anti-rabbit IgGs (Invitrogen) for 30 min at room temperature and were finally counterstained with DAPI. Imaging was carried out as above.

TUNEL staining was carried out with de-paraffinized sections using the Apoptag Red In Situ Apoptosis Detection Kit S7165 (Millipore). Sections were treated with 20 μg/ml proteinase K for 15 min at room temperature to de-mask nuclear material. After incubation with equilibration buffer, slides were incubated with TdT enzyme for 1 hr at 37°C. After rinsing, slides were incubated with anti-digoxigenin rhodamine antibodies for 30 minutes at room temperature and were then were counterstained with DAPI.

Micro-computed tomography

Embryos and embryo parts were fixed in buffered 4% paraformaldehyde overnight at 4°C, rinsed and subjected to micro computed tomography (μCT) using a μCT40 SCANCO Medical system. Samples were scanned using a 36 mm holder at 45 kvolts of energy, 12 μm scanning thickness and medium resolution. Two dimensional slice images were selected and used to generate three-dimensional reconstructions with the following parameters: filter width sigma = 0.8, support level = 1.0, and threshold =173. The same values were used to analyze wild type and mutant samples at each specified time point. Three-dimensional images were rotated at specific angles to generate lateral and bird-eye views.

Results

Global skeletal consequences of conditional Ext1 deletion and HS production

We first assessed the consequences of conditional *Ext1* ablation on overall skeletal development and growth. To this end, *Ext1*$^{f/f}$ mice were mated with *Gdf5-Cre* mice in which Cre-recombinase expression patterns closely mimic those of endogenous *Gdf5* in developing limb synovial joints, fibrous/synovial intervertebral joints and other tissues and organs including ears and tendons (Rountree et al., 2004). Gross anatomical inspection at P0 showed that the compound *Gdf5-Cre;Ext1*$^{f/f}$ mice were slightly smaller (Fig. 1E) than control *Ext1*$^{f/f}$ littermates (hereafter referred to as wild type) (Fig. 1A) and occasionally displayed mild syndactyly particularly of digits 1 and 2 (Figs. 1B, F, arrowhead). Analysis by μCT revealed that skeletal development and growth were delayed in the mutants and their trunk and limb elements were hypomorphic and slightly mis-oriented (Figs. 1G–H) compared to controls (Figs. 1C–D). The hypomorphic phenotype of mutant vertebral bodies was more obvious at higher magnification (Fig. 1G, inset). Mutant mice all died at birth of respiratory failure. No appreciable changes in limbs, trunk and body length were observed in heterozygous *Gdf5-Cre;Ext1*$^{f/+}$ mice that were all viable and seemingly normal (not shown).

To verify that *Gdf5-Cre* had acted selectively and locally in both limbs and spine, we mated the *Gdf5-Cre* mice with *Rosa R26R* mice. As expected, *LacZ* activity was restricted to limb synovial joints and cells but was absent in underlying epiphyseal chondrocytes (Figs. 1I–K) (Koyama et al., 2008; Rountree et al., 2004). Interestingly, it was particularly strong in the anterior autopod region (Fig. 1I, arrowhead) suggesting that *Ext1* could have been broadly ablated in that region and may have led to anterior syndactyly by affecting Sonic hedgehog signaling and reducing Gli3R production (Towers and Tickle, 2009) (Fig. 1F, arrowhead). In intervertebral joints, the *LacZ*-positive cells were restricted to the annulus fibrosus (*af*) (Figs. 1LM), but were essentially absent in nucleus pulposus (*np*) cells and adjacent cartilaginous vertebral bodies (Fig. 1L) (Iwamoto et al., 2007).

To demonstrate that *Gdf5-Cre* action had resulted in local reductions in *Ext1* expression and HS levels, longitudinal sections of long bone anlagen from E16.5 *Gdf5-Cre;Ext1*$^{f/f}$ and control *Ext1*$^{f/f}$ mice were processed for qualitative analysis of HS presence and distribution by immunostaining (David et al., 1992). In controls, HS staining was strong throughout much of the limb cartilaginous anlagen (Figs. 2A–B) including articulating and epiphyseal regions (Figs. 2DE), and throughout the intervertebral joints (Figs. 2F–G). In *Gdf5-Cre;Ext1*$^{f/f}$ mutants, there was a selective and restricted reduction of HS staining in limb joint area (Figs. 2H–I, K–L) and annulus fibrosus (Fig. 2M–N, arrows), but staining elsewhere was virtually indistinguishable from that in controls. In situ hybridization confirmed that *Ext1* transcripts were clear over the entire epiphyseal and metaphyseal regions of control limb anlagen (Fig. 2C), but were selectively reduced in the joint area of *Gdf5-Cre;Ext1*$^{f/f}$ mutants (Fig. 2J).

Joint surface and epiphyseal region are deranged in conditional Ext1 mutant limbs

To assess the consequences of conditional *Ext1* deficiency on structure, phenotypic expression and organization of developing limb synovial joints, serial sections of humeri from E16.5 and P0 *Gdf5-Cre;Ext1*$^{f/f}$ mice and control *Ext1*$^{f/f}$ littermates were stained with safranin O-fast green to analyze their cartilaginous and non-cartilaginous tissue components. In controls, joints such as the shoulder joint were well formed and displayed typical interlocking concave and convex shapes on scapula (*sc*) and humerus (*hu*), a clear synovial cavity and a conspicuous joint capsule (Figs. 3A, O). The cartilaginous skeletal elements stained strongly with safranin-O reflecting their high proteoglycan content, and the cells lining the articulating surface zone had a typical flat and mesenchymal shape at both stages and were tightly packed, reflecting their role to create a smooth, continuous, anti-adhesive and mechanically-suitable tissue structure (Figs. 3B, P, arrowheads). In *Gdf5-Cre;Ext1*$^{f/f}$ mutants the overall organization and structure of the joints were not markedly altered (Figs. 3H, V). However, there were clear and consistent defects in the articulating layer that had become hypocellular and displayed gaps in its surface continuity (Figs. 3I, W, arrowheads). In addition, the average diameter of the subadjacent epiphyseal chondrocytes was larger and thus atypical (Figs. 3I, W) compared to control (Figs. 3B, P).

We carried out gene expression analyses to define the cellular phenotypes. At both E16.5 and P0, the articular superficial zone was characterized by strong expression of *lubricin* (Figs. 3C, Q), an anti-adhesive mucin-like protein that is critical for establishment and maintenance of articular surface friction-less character (Jay et al., 2001), and by *collagen IIA* expression (Figs. 3D, R) (Nalin et al., 1995). As expected, *matrillin-1* expression was minimal in superficial zone cells (Figs. 3E, S, brackets), but was strong in subadjacent epiphyseal chondrocytes (Hyde et al., 2007), and mature and cartilage-characteristic *collagen IIB* was a major expression product of all chondrocytes (Figs. 3F, T). In the mutant joints, *lubricin* gene expression was clearly substandard at E16.5 and was absent in much of the superficial zone by P0 (Figs. 3J, X, arrowheads), but was ectopically and randomly expressed within the epiphyseal region (Figs. 3J, X, arrows). Similarly, *collagen IIA* transcripts were no longer limited to the superficial zone, but were ectopically expressed in epiphyseal area (Figs. 3K, Y, arrowheads). Interestingly, there was a concurrent and reciprocal decrease in expression of *matrillin-1* over the same area (Figs. 3L, Z1). Transcripts for *collagen IIB* remained largely unchanged and abundant suggesting that there was no obvious overall loss of chondrocyte differentiated phenotype (Figs. 3M, Z2). There was also no ectopic expression of *Indian hedgehog* and *collagen X*, markers of prehypertrophic and hypertrophic chondrocytes, respectively, and their transcripts were observed only at prescribed locations within metaphyseal growth plates (Supplementary Fig. 1 and Figs. 3G, N, U, Z3, arrows). The latter findings suggest that despite increased cell size and deranged behavior, the mutant epiphyseal chondrocytes had not actually progressed to a hypertrophic status. On the other hand, the data indicate that mutant superficial zone cells and epiphyseal chondrocytes no longer had the capacity to maintain their distinct locations, phenotype and developmental characteristics and became intermingled.

Mutant epiphyses display increased apoptosis and abnormal proliferation patterns

To account for the hypocellular nature of articular superficial zone in mutants, we asked whether it might involve increased cell death. Indeed, TUNEL staining showed that there was an appreciable number of positive cells on the articulating surface of *Gdf5-Cre;Ext1*$^{f/f}$ mutant long bones such as the humerus (Fig. 4D–F), but no TUNEL-positive cells were appreciable in controls (Figs. 4A–C). Next, we analyzed cell proliferation by determining the gene expression patterns of the mitotic marker histone 4C (H4C). In control E16.5 skeletal elements, *H4C*-positive cells were widely distributed and occupied the superficial zone and cartilaginous epiphyseal areas (Figs. 5A–B, E–F). By P0, there were still numerous

H4C-positive cells in the superficial zone and adjacent cells, but there was a significant drop in such cells in the center of the epiphyseal area (Figs. 5G–H, K–L) reflecting onset of secondary ossification center formation (Figs. 5G–H, circled area). We observed slight and statistically significant decreases in proliferation patterns and index in mutants at E16.5 (Figs. 5C–D, E–F). In P0 mutant humeri, however, there was a marked decrease in proliferation within, and immediately adjacent to, the superficial zone, while there was ectopic proliferation in a more central epiphyseal area (Figs. 5I–J, K–L), confirming that superficial zone and epiphyseal end had become phenotypically deranged and intermingled and indicating that formation of the secondary ossification center wasdelayed. Similar data were obtained in zeugopod elements (not shown).

Autopod joint formation is severely altered in mutants

Autopod synovial joints share many if not most characteristics with more proximal limb joints, but previous studies have indicated that they are more sensitive to loss-of-function mutations in HS-binding factors such as BMP family members (Storm and Kingsley, 1996). Thus, it became of interest to determine the degree to which digit joint formation was affected in *Gdf5-Cre;Ext1*$^{f/f}$ mutants. Safranin O-fast green staining showed that the cartilaginous phalangeal elements were hypomorphic and developmentally delayed in the mutants (Figs. 6F, Q) compared to controls (Figs. 6A, K), as revealed by absence of a primary ossification center (Fig. 6Q, arrow) that was well formed in controls (Fig. 6K, arrow). The interphalangeal joints were severely affected in mutants, were ill defined morphologically and displayed even partial fusion (Figs. 6F, Q, arrowheads), while control joints were well organized and displayed a clear articulating superficial zone (Figs. 6A, K, arrowheads). Indeed, while gene expression of interzone and joint markers *Gdf5, Erg, collagen IIA* and *lubricin* was strong and distinct in controls (Figs. 6B–E), expression was negligible in the most affected and largely fused mutant joints (Figs. 6G–J). In such joints, there was increased BMP signaling as indicated by pSmad1/5/8 distribution (Fig. 6S) and reduced expression of *Patched1* and *Gli3* (Fig. 6T–U) compared to controls (Fig. 6L–O), suggesting that coordination between BMP and Ihh signaling had been disrupted. Indeed, *Ihh* expression itself was extremely low in these mutant digits (Fig. 6V) compared to control (Fig. 6P) and could have caused joint fusion (St-Jacques et al., 1999).

Intervertebral joint formation and organization depend on Ext1 expression

To test whether other types of joints depend on *Ext1* expression, we extended our analysis to the fibrous-synovial intervertebral joints that are structurally more complex than limb joints. By P0, each joint displayed a typical intervertebral disc composed of an annulus fibrosus (that expresses *Gdf5* as shown in Fig. 1M) and a gelatinous nucleus pulposus (Figs. 7A, C). Each disc faced, and articulated with, the synovial endplates (*ep*) of flanking vertebra containing their typical flat-shaped cells (Figs. 7C–D). Both the annulus fibrosus and endplates stained less intensely with Safranin-O (Figs. 7C–D) and expressed much less *matrillin-1* (Figs. 7D–E) than the adjacent cartilaginous portions of the vertebrae, thus mimicking the phenotypic characteristics of limb joint superficial zone. Indeed, annulus fibrosus and endplate cells specifically expressed *lubricin* (Fig. 7G). All these structural and organizational features were markedly affected in the *Gdf5-Cre;Ext1*$^{f/f}$ mutants. Some intervertebral joints were missing and the adjacent vertebrae had fused as shown by the patterns of Safranin-O staining (Fig. 7H, arrowhead) and *collagen II* expression patterns (Fig. 7I, arrowhead) compared to controls (Figs. 7A–B). When disc remnants were present, they contained ill-defined and hypocellular annulus fibrosus and endplates (Fig. 7J) that barely expressed *lubricin* (Fig. 7N). Many of the cells present were round (Figs. 7K, M) rather than flat-shaped as in controls (Figs. 7D, F) and expressed *matrillin-1* adjacent to the nucleus pulposus (Fig. 7L), indicating that the mutant cells were expressing traits of vertebral body chondrocytes rather than endplate characteristics.

As pointed out above, joint ablation and fusion have been demonstrated in limb and spine joints as a consequence of natural and experimental gain- or loss-of-function mutations or manipulations of BMP gene expression and signaling (Brunet et al., 1998; Merino et al., 1999). In addition, limb joint fusion was observed following conditional *Col2a1-Cre*-driven ablation of *β-catenin* or *Wnt* family members (Mak et al., 2006; Spater et al., 2006). To determine whether similar Wnt/β-catenin signaling mechanisms operate in intervertebral joint development, we created and analyzed the intervertebral joints of *Col2a1-Cre; β-catenin*$^{f/f}$ mice. Indeed, we observed extensive joint fusion in E18.5 mutants revealed by histological staining and *collagen II* expression patterns (Figs. 8H, I, arrowheads) absent in controls (Figs. 8A, B). When present in mutants, the annulus fibrosus contained oval-round cells (Figs. 8J–K) rather than elongated cells (Figs. 8C–D). Compared to controls (Figs. 8E–F), many of the mutant cells lacked *lubricin* transcripts (Fig. 8M) but expressed *matrillin-1* (Fig. 8L) as seen above (Fig. 7L), strengthening the conclusion that the cells expressed traits of vertebral body chondrocytes and were intermingled with dwindling endplate cells. These severe gene expression alterations were selective and restricted to the joints since surrounding connective tissues expressed *collagen I* in both WT and mutants (Figs. 8G, N).

Discussion

The study provides novel evidence that local ablation of *Ext1* and consequent local drop in HS production cause extensive derangement of joint formation in both limbs and spine. The limb joints between stylopod and zeugopod skeletal elements do form in the *Gdf5-Cre;Ext1*$^{f/f}$ mutants, but come to display a defective superficial zone with substandard *lubricin* expression, cell death and histological gaps interrupting their normally continuous articulating surface. The more distal autopod joints between phalangeal elements are more severely affected and are often ablated, resulting in fusion of opposing cartilaginous skeletal elements. This is in keeping with previous studies showing that though limb joints obey similar overall developmental mechanisms, the autopod joints are more vulnerable and more severely affected by gene manipulations (Storm and Kingsley, 1996). Severe defects and even joint fusion occur also in the spine of *Gdf5-Cre;Ext1*$^{f/f}$ mice where the intervertebral discs are often missing and when present, display substandard and non-functional features. Thus, local production of HS chains and HSPGs represents is a required step for progression of joint formation at many, if not all, anatomical locations.

Our data indicate that local loss of *Ext1* expression affected a number of essential joint formation mechanisms. Chief among them is the fine balance of chondrogenic and anti-chondrogenic mechanisms that are required for initial formation of the mesenchymal interzone and for developmental progression of its cells to eventually produce chondrogenic structures such as articular cartilage and non-chondrogenic structures such as intra-joint ligaments, synovial lining and inner capsule (Pacifici et al., 2005). We have shown previously that these structures all derive from the initial population of *Gdf5*-expressing interzone cells (Koyama et al., 2007a; Koyama et al., 2008; Rountree et al., 2004). It is thus likely that by being required binding and functional partners of many such factors, HSPGs would have the essential role of determining their diffusion and distribution patterns and influencing chondrogenic versus anti-chondrogenic action on prescribed targets within and immediately surrounding the developing interzone and joint. This interpretation fits well with our observation that *Ext1* ablation is associated with ectopic BMP signaling and lack of Gli3 expression; these combined changes could have tilted the balance toward chondrogenesis causing joint derangement and fusion in digits (Fig. 6). Thus, the data indicate that one important and possibly critical function of HSPGs within developing joints is to initially favor anti-chondrogenic mechanisms and establish the mesenchymal character of the interzone. In keeping with this conclusion, fusion of certain joints was observed in double mutant mice lacking *Wnt9a* and *Wnt4* (Spater et al., 2006) and in mice carrying a

hypomorphic *Ext1* allele (Koziel et al., 2004). It agrees also with joint defects seen after ablation of *JAWS* that encodes a Golgi-associated protein involved in glycosaminoglycan sulfation (Sohaskey et al., 2008) or after over-expression of *Sulf1*, a sulfatase specifically expressed during skeletogenesis that catalyzes the removal of 6-O sulfate groups from HS-PGs (Zhao et al., 2006). In particular, ectopic *Sulf1* over-expression and consequent excessive loss of sulfation led to excessive chondrogenesis and fusion of limb joints. Though these possibilities are plausible and attractive, HSPGs could also regulate other joint cell characteristics and functions such as cell shape, cell-cell and cell-matrix interactions and cell survival as seen in other systems (Bernfield et al., 1999; Hacker et al., 2005). Indeed we show that the mutant *Ext-1*-deficient joints display cell death and an abnormal superficial zone that is uneven and contains rounder and more dispersed cells rather than normal flat and con-joined cells. Lastly, HSPGs could be required to mediate interactions with factors that influence expression of specific phenotypic traits of joint cells. For instance, the HS-binding factor TGFβ1 has been shown to boost *lubricin* gene expression in joint cells (Jones and Flannery, 2007), and TGFβ signaling and local expression of TGFβ receptors have important roles in joint formation and maintenance (Serra et al., 1997; Spagnoli et al., 2007). Substandard local action of TGFβ1 in the *Gdf5-Cre;Ext1*$^{f/f}$ mutants could have caused substandard *lubricin* expression, excessive surface abrasion and superficial cell death and/or dislodging by muscle-driven movement that participates in joint formation (Kahn et al., 2009;Pitsillides, 2006). In sum, the normal initiation and progression of the joint formation process require multiple specific local events and mechanisms that are directly or indirectly dependent on the presence and functioning of HSPGs.

Intervertebral joints differ in many respects from limb joints and most clearly in their structure. There is wide agreement that the nucleus pulposus cells derive directly from the notochord, though it is not clear how the notochord becomes segmented to produce individual nuclei pulposi and how it is eliminated from within the body of the developing vertebrae (Verbout, 1985). There is also long standing evidence that each vertebral body is produced by sclerotomal cells that migrate from the posterior and anterior halves of adjacent somites and converge ventrally to form the corresponding vertebra (Watterson et al., 1954). What remains less clear is where the annulus fibrosus-forming cells come from. Theoretically, the cells could simply be a portion of sclerotomal cells that chance to become anatomically located in the appropriate annulus-forming area. Recently, Christ and collaborators used microsurgical approaches to determine more precisely the origin of annulus fibrosus progenitor cells (Christ et al., 2004; Mattipalli et al., 2005). Interestingly, they found that removal of somitocoele cells led to absence of annulus fibrosus formation and to joint fusion. The cells (they named arthrotome) would represent a pre-specified cohort of somitic cells with annulus fibrosus-forming capacity, while sclerotome cells would be pre-specified to give rise to the vertebral body and endplates only. In these respects, the arthrotome cells would behave and function similarly to interzone cells that we have shown to be responsible for limb joint formation (Koyama et al., 2007a; Koyama et al., 2008). This would imply that every joint in the organism is the product of specialized cohorts of joint-specific progenitor cells that initially express *Gdf5* and go on to eventually express *Erg, lubricin* and other unique joint genes. Given the above observations and considerations, the severe aberrations in intervertebral joints and frequent fusion we observe in *Gdf5-Cre;Ext1*$^{f/f}$ mutants could be due to a failure of somitocoele-derived cells to migrate or thrive. As in the case of limb joints, it is also possible that fusion could be due to excessive signaling by chondrogenic factors and reduced signaling by anti-chondrogenic factors. Indeed, our data show that vertebral fusion also occurred after conditional ablation of *β-catenin* and consequent decrease of the otherwise powerful anti-chondrogenic Wnt/β-catenin signaling ability (Day et al., 2005).

In closing, it is important to note that the overall lengthening and primary ossification of the *Gdf5-Cre;Ext1*$^{f/f}$ mutant long bones were slightly delayed in stylopod and zeugopod and severely delayed in digits. As our data indicate (Fig. 5), the reduction in longitudinal growth is likely due to the fact that the patterns of chondrocyte proliferation are significantly altered in mutant epiphyses. In controls, proliferation normally characterizes the entire epiphysis at early stages, but then drops in the central region (as it evolves into a secondary ossification center) and is maintained in both the superficial articulating region and the incipient proliferative zone of metaphyseal-diaphyseal growth plate (Naski et al., 1998). In the mutants, these distinct and dynamic proliferation patterns are disrupted, and this is accompanied by a seemingly random distribution of, and intermingling amongst, *lubricin-*, *Gdf5*, *collagen IIA* and *Erg*-expressing epiphyseal chondrocytes, strongly indicating that the developmental definition and roles of the entire epiphyseal region were disrupted. Such encompassing defects could have rendered ineffective the normal mechanisms that regulate chondrocyte proliferation and renewal such as those controlled by the Ihh-PTHrP axis (Kronenberg, 2003). It is however, more difficult at the moment to account for the delays in primary ossification that could arise from indirect mechanisms. Ongoing experiments should provide answers to these important questions.

Supplementary Material

Refer to Web version on PubMed Central for supplementary material.

Acknowledgments

We would like to thank Dr. R.P. Boot-Handford for providing a mouse matrillin-1 cDNA clone. This study was supported by grants from the National Institutes of Health 5RO1AG025868 and 5RO1AR046000 (M.P.) and 1RC1AR058382 (M.P. and E.K.).

References

Albrecht AN, Schwabe GC, Striker S, Boddrich A, Wanker EE, Mundllos S. The synpolydactyly homolog (spdh) mutation in the mouse - a defect in patterning and growth of limb cartilage elements. Mech. Dev 2002;112:53–67. [PubMed: 11850178]

Andersen H. Histochemical studies on the histogenesis of the knee joint and superior tibio-fibular joint in human fetuses. Acta Anat 1961;46:279–303. [PubMed: 13861166]

Archer CW, Dowthwaite GP, Francis-West P. Development of synovial joints. Birth Defects Research, Pt. C 2003;69:144–155.

Arikawa-Hirasawa E, Watanabe H, Takami H, Hassell JR, Yamada Y. Perlecan is essential for cartilage and cephalic development. Nature Genet 1999;23:354–358. [PubMed: 10545953]

Bernfield M, Gotte M, Park PW, Reizes O, Fitzgerald ML, Lincecum J, Zako M. Functions of cell surface heparan sulfate proteoglycans. Annu. Rev. Biochem 1999;68:729–777. [PubMed: 10872465]

Bishop JR, Schuksz M, Esko JD. Heparan sulphate proteoglycans fine-tune mammalian physiology. Nature 2007;446:1030–1037. [PubMed: 17460664]

Brunet LJ, McMahon JA, McMahon AP, Harland RM. Noggin, cartilage morphogenesis, and joint formation in the mammalian skeleton. Science 1998;280:1455–1457. [PubMed: 9603738]

Christ B, Huang R, Scaal M. Formation and differentiation of the avian sclerotome. Anat. Embryol 2004;208:333–350. [PubMed: 15309628]

David G, Bai XM, van der Schueren B, Cassiman J-J, van der Berghe H. Developmental changes in heparan sulfate expression: in situ detection with mAbs. J. Cell Biol 1992;119:961–975. [PubMed: 1385449]

Day TF, Guo X, Garrett-Beal L, Yang Y. Wnt/β-catenin signaling in mesenchymal progenitors controls osteoblast and chondrocyte differentiation during vertebrate skeletogenesis. Dev. Cell 2005;8:739–750. [PubMed: 15866164]

Esko JD, Selleck SB. Order out of chaos: assembly of ligand binding sites in heparan sulfate. Annu. Rev. Biochem 2002;71:435–471. [PubMed: 12045103]

Hacker U, Nybakken K, Perrimon N. Heparan sulphate proteoglycans: the sweet side of development. Nature Rev. Mol. Cell Biol 2005;6:530–541. [PubMed: 16072037]

Holder N. An experimental investigation into the early development of the chick elbow joint. J. Embryol. Exp. Morphol 1977;39:115–127. [PubMed: 886251]

Hyde G, Dover S, Aszodi A, Wallis GA, Boot-Handford RP. Lineage tracing using matrilin-1 gene expression reveals that articular chondrocytes exist as the joint interzone forms. Dev. Biol 2007;304:825–833. [PubMed: 17313942]

Inatani M, Irie F, Plump AS, Tessier-Lavigne M, Yamaguchi Y. Mammalian brain morphogenesis and midline axon guidance require heparan sulfate. Science 2003;302:1044–1046. [PubMed: 14605369]

Iwamoto M, Tamamura Y, Koyama E, Komori T, Takeshita N, Williams JA, Nakamura T, Enomoto-Iwamoto M, Pacifici M. Transcription factor ERG and joint and articular cartilage formation during mouse limb and spine skeletogenesis. Dev. Biol 2007;305:40–51. [PubMed: 17336282]

Jay GD, Tantravahi U, Britt DE, Barrach HJ, Cha CJ. Homology of lubricin and superficial zone protein (SZP): products of megakaryocyte stimulating factor (MSF) gene expression by human synovial fibroblasts and articular chondrocytes localized to chromosome 1q25. J. Orthop. Res 2001;19:677–687. [PubMed: 11518279]

Jones ARC, Flannery CR. Bioregulation of lubricin expression by growth factors and cytokines. Eur. Cells Materials 2007;13:40–45.

Kahn J, Shwartz Y, Blitz E, Krief S, Sharir A, Breitel DA, Rattenbach R, Relaix F, Maire P, Roundtree RB, Kingsley DM, Zelzer E. Muscle contraction is necessary to maintain joint progenitor cell fate. Dev. Cell 2009;16:734–743. [PubMed: 19460349]

Koyama E, Golden EB, Kirsch T, Adams SL, Chandraratna RAS, Michaille J-J, Pacifici M. Retinoid signaling is required for chondrocyte maturation and endochondral bone formation during limb skeletogenesis. Dev. Biol 1999;208:375–391. [PubMed: 10191052]

Koyama E, Ochiai T, Rountree RB, Kingsley DM, Enomoto-Iwamoto M, Iwamoto M, Pacifici M. Synovial joint formation during mouse limb skeletogenesis. Roles of Indian hedgehog signaling. Ann. N.Y. Acad. Sci 2007a;1116:100–112. [PubMed: 18083924]

Koyama E, Shibukawa Y, Nagayama M, Sugito H, Young B, Yuasa T, Okabe T, Ochiai T, Kamiya N, Rountree RB, Kingsley DM, Iwamoto M, Enomoto-Iwamoto M, Pacifici M. A distinct cohort of progenitor cells participates in synovial joint and articular cartilage formation during mouse limb skeletogenesis. Dev. Biol 2008;316:62–73. [PubMed: 18295755]

Koyama E, Young B, Nagayama M, Shibukawa Y, Enomoto-Iwamoto M, Iwamoto M, Maeda Y, Lanske B, Song B, Serra R, Pacifici M. Conditional Kif3a ablation causes abnormal hedgehog signaling topography, growth plate dysfunction, and excessive bone and cartilage formation during mouse skeletogenesis. Development 2007b;134:2159–2169. [PubMed: 17507416]

Koziel L, Kunath M, Kelly OG, Vortkamp A. Ext1-dependent heparan sulfate regulates the range of Ihh signaling during endochondral ossification. Dev. Cell 2004;6:801–813. [PubMed: 15177029]

Kronenberg HM. Developmental regulation of the growth plate. Nature 2003;423:332–336. [PubMed: 12748651]

Lin X. Functions of heparan sulfate proteoglycans in cell signaling during development. Development 2004;131:6009–6021. [PubMed: 15563523]

Lobe CG, Koop KE, Kreppner W, Lomeli H, Gertsenstein M, Nagy A. Z/AP, a double receptor for Cre-mediated recombination. Dev. Biol 1999;208:281–292. [PubMed: 10191045]

Mak KK, Chen M-H, Day TF, Chuang P-T, Yang Y. Wnt/β-catenin signaling interacts differentially with Ihh signaling in controlling endochondral bone and synovial joint formation. Development 2006;133:3695–3707. [PubMed: 16936073]

Mattipalli VR, Huang R, Patel K, Christ B, Scaal M. Arthrotome: a specific joint forming compartment in the avian somite. Dev. Dyn 2005;234:48–53. [PubMed: 16028274]

Merino R, Macias D, Ganan Y, Economides AN, Wang X, Wu Q, Stahl N, Sampath TK, Varona P, Hurle JM. Expression and function of Gdf-5 during digit skeletogenesis in the embryonic chick leg bud. Dev. Biol 1999;206:33–45. [PubMed: 9918693]

Mitrovic D. Development of the diathrodial joints in the rat embryo. Am. J. Anat 1978;151:475–485. [PubMed: 645613]

Nalin AM, Greenlee TK, Sandell LJ. Collagen gene expression during development of avian synovial joints: transient expression of type II and XI collagen genes in the joint capsule. Dev. Dyn 1995;203:352–362. [PubMed: 8589432]

Namimatsu S, Ghazizadeh M, Sugisaki Y. Reversing the effects of formalin fixation with citraconic anhydride and heat: a universal antigen retrieval method. J. Histochem. Cytochem 2005;53:3–11. [PubMed: 15637333]

Naski MC, Colvin JS, Coffin JD, Ornitz DM. Repression of hedgehog signaling and BMP4 expression in growth plate cartilage by fibroblast growth factor receptor 3. Development 1998;125:4977–4988. [PubMed: 9811582]

Ovchinnikov DA, Deng JM, Ogunrinu G, Behringer RR. Col2a1-directed expression of Cre recombinase in differentiating chondrocytes in transgenic mice. Genesis 2000;26:145–146. [PubMed: 10686612]

Pacifici M, Koyama E, Iwamoto M. Mechanisms of synovial joint and articular cartilage formation: recent advances, but many lingering mysteries. Birth Defects Research, Pt. C 2005;75:237–248.

Pitsillides AA. Early effects of embryonic movement: "a shot out of the dark". J. Anat 2006;208:417–431. [PubMed: 16637868]

Rountree RB, Schoor M, Chen H, Marks ME, Harley V, Mishina Y, Kingsley DM. BMP receptor signaling is required for postnatal maintenance of articular cartilage. PLoS Biology 2004;2:1815–1827.

Serra R, Johnson M, Filvaroff EH, LaBorde J, Sheehan DM, Derynck R, Moses HL. Expression of a truncated, kinase-defective TGF-β type II receptor in mouse skeletal tissue promotes terminal chondrocyte differentiation and osteoarthritis. J. Cell Biol 1997;139:541–552. [PubMed: 9334355]

Shibukawa Y, Young B, Wu C, Yamada S, Long F, Pacifici M, Koyama E. Temporomandibular joint formation and condyle growth require Indian hedgehog signaling. Dev. Dyn 2007;236:426–434. [PubMed: 17191253]

Shimo T, Gentili C, Iwamoto M, Wu C, Koyama E, Pacifici M. Indian hedgehog and syndecan-3 coregulate chondrocyte proliferation and function during chick limb skeletogenesis. Dev. Dyn 2004;229:607–617. [PubMed: 14991716]

Sohaskey ML, Yu J, Diaz MA, Plaas AH, Harland RM. JAWS coordinates chondrogenesis and synovial joint positioning. Development 2008;135:2215–2220. [PubMed: 18539921]

Soriano P. Generalized lacZ expression with the ROSA26 Cre reporter strain. Nat. Genet 1999;21:70–71. [PubMed: 9916792]

Spagnoli A, O'Rear L, Chandler RL, Granero-Molto F, Mortlock DP, Gorska AE, Weis JA, Longobardi L, Chytil A, Shimer K, Moses HL. TGF-β signaling is essential for joint morphogenesis. J. Cell Biol 2007;177:1105–1117. [PubMed: 17576802]

Spater D, Hill TP, Gruber M, Hartmann C. Role of canonical Wnt-signaling in joint formation. Eur. Cells Materials 2006;12:71–80.

St-Jacques B, Hammerschmidt M, McMahon AP. Indian hedgehog signaling regulates proliferation and differentiation of chondrocytes and is essential for bone formation. Genes Dev 1999;13:2076–2086.

Storm EE, Kingsley DM. Joint patterning defects caused by single and double mutations in members of the bone morphogenetic protein (BMP) family. Development 1996;122:3969–3979. [PubMed: 9012517]

Towers M, Tickle C. Growing models of vertebrate limb development. Development 2009;136:179–190. [PubMed: 19103802]

Verbout A. The development of the vertebral column. Adv. Anat. Embryol. Cell Biol 1985;90:1–122. [PubMed: 3969844]

Viviano BL, L S, Pflederer C, Paine-Saunders S, Mills K, Saunders S. Altered hematopoiesis in glypican-3-deficient mice results in decreased osteoclast differentiation and a delay in endochondral ossification. Dev. Biol 2005;282:152–162. [PubMed: 15936336]

Watterson R, Fowler I, Fowler B. The role of the neural tube and notochord in development of the axial skeleton of the chick. Am. J. Anat 1954;95:337–397. [PubMed: 14349892]

Zhao W, Sala-Newby GB, Dhoot GK. Sulf1 expression pattern and its role in cartilage and joint development. Dev. Dyn 2006;235:3327–3335. [PubMed: 17061267]

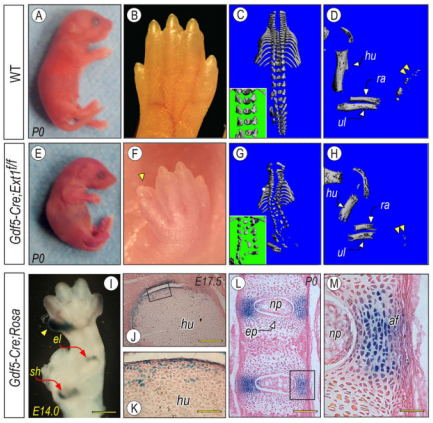

Fig. 1.

Phenotypic characterization of *Gdf5-Cre;Ext1*$^{f/f}$ mutant mice. (A–H) Compared to P0 wild type (WT) littermates (A–D), the mutant mice exhibit overall growth retardation (E), mild syndactyly of anterior digits (F), aberrant vertebral development (G, inset) and reduced growth of stylopod and zeugopod skeletal elements and digits (H, double arrowhead) appreciable by μCT. (I–M) Histochemical detection of *LacZ* activity in *Gdf5-Cre;RosaR26R* mice. Note that reporter activity is restricted to prescribed joint sites (I) and articulating layer (J–K) in developing limbs and to the annulus fibrosus (*af*) in the developing spine. Note also the strong reporter activity in the anterior autopod region, but it is not clear whether this relates to anterior syndactyly seen in mutants. *hu*, humerus; *ra*, radius; *ul*, ulna; *el*, elbow; *sh*, shoulder; *np*, nucleus pulposus; *ep*, endplate. Scale bars: 1 mm in I; 200 μm in J; 70 μm in K; 100 μm in L; 50 μm in M.

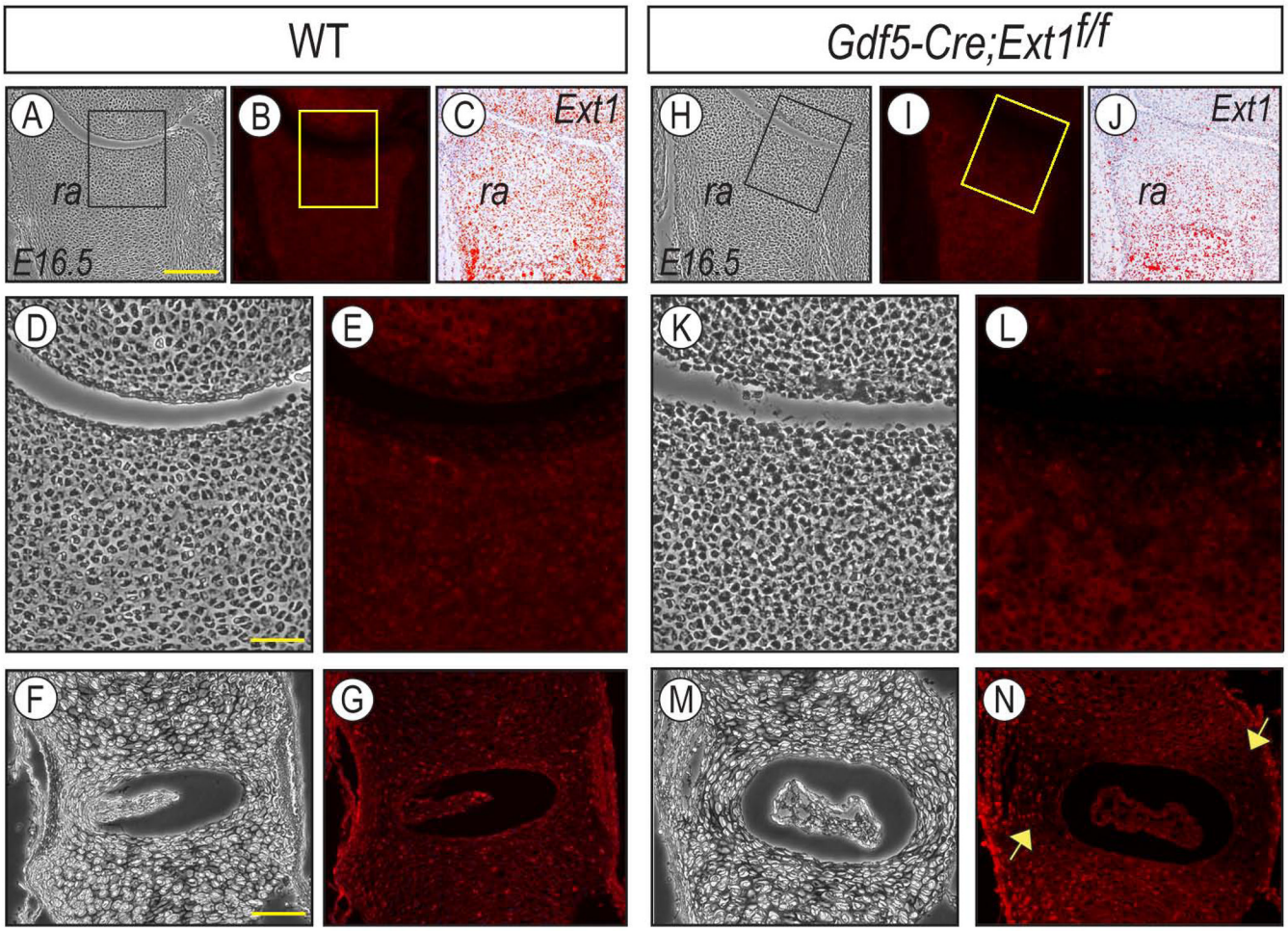

Fig. 2.

HS levels and *Ext1* expression are selectively reduced in mutant joints. (A–B, D–E) HS chains are abundant in WT E16.5 cartilaginous radius as revealed by immunohistochemistry (B, E). Boxed areas in A–B are shown at higher magnification in D–E, respectively. (C) *Ext1* transcripts are abundant in cartilaginous radius as revealed by in situ hybridization. (F–G) HS immunostaining is strong in intervertebral joints. (H–I, K–L) HS levels are specifically reduced in the joint area in *Gdf5-Cre;Ext1*$^{f/f}$ mice (I, L) as are *Ext1* transcripts (J). Boxed areas in H–I are shown at higher magnification in K–L. (M–N) HS immunostaining is selectively reduced in annulus fibrosus in *Gdf5-Cre;Ext1*$^{f/f}$ mice (arrows). *ra*, radius. Scale bars: 250 μm for A–C and H–J; 100 μm for D–E and K–L; and 175 μm for F–G and M–N.

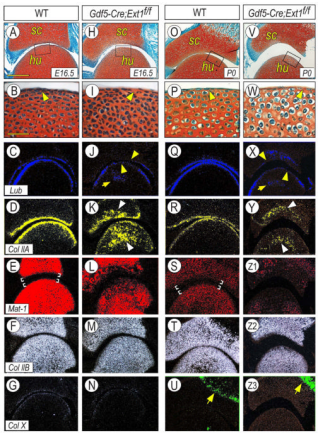

Fig. 3.

Superficial zone and epiphyseal end of proximal limb long bones are defective in mutants. (A–Z3) Compared to WT E16.5 and P0 shoulder joints (A–G, O–U), the mutant *Gdf5-Cre;Ext1*$^{f/f}$ joints exhibit histological gaps in their articulating superficial zone (I, W, arrowheads) and cell enlargement (W) both revealed by Safranin-O/fast green staining. They also display reduced lubricin (*Lub*) expression in superficial zone (J, X, arrowheads), aberrant and ectopic *collagen IIA (Col IIA)*, *matrilin-1 (Mat-1)* and *lubricin* expression in epiphyseal area (K, Y, arrows), and fairly normal *collagen IIB (Col IIB)* expression (M, Z2) all revealed by in situ hybridization. Despite abnormal cell enlargement, the mutant epiphyseal chondrocytes do not express *collagen X* (N, Z3) that is restricted to its prescribed hypertrophic zone in the metaphyseal growth plates in both WT and mutant elements at P0 (G, N, U, Z3, arrows). Boxed areas in A, H, O and V are shown at higher magnification in B, I, P and W, respectively. Brackets in E and S demarcate the superficial zone that does not express *matrillin-1*. *Sc*, scapula; *hu*, humerus. Scale bars: 250 μm in A, C–G, H, J–N, O, Q–U, V, X–Z3; 75 μm in B, I, P, W.

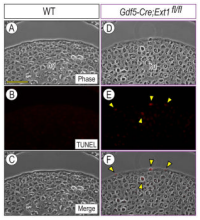

Fig. 4.

Mutant superficial zone contains apoptotic cells. Serial longitudinal sections from P0 WT and *Gdf5-Cre;Ext1*$^{f/f}$ limbs processed for TUNEL staining. TUNEL-positive cells are not detectable in epiphyseal end of WT humerus (*hu*) (A–B), but several such positive cells are present in mutant humerus and are largely restricted to the articulating surface (D–E). Merged images are shown in (C, F). Scale bar: 100 μm for A–F.

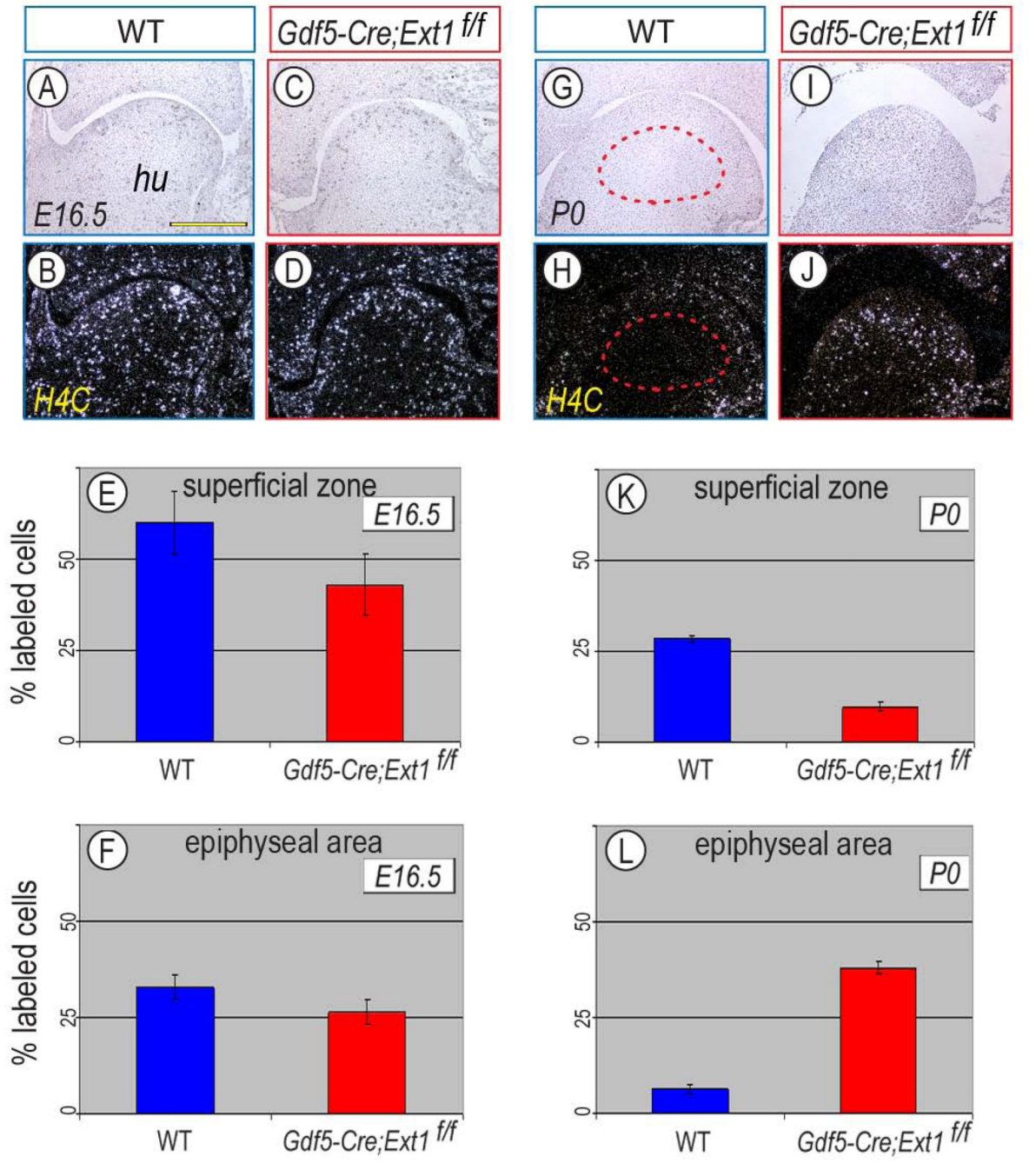

Fig 5.

Proliferation patterns are deranged in mutant epiphyses. (A–F) At E16.5, *H4C*-expressing proliferative cells are located in both articulating superficial zone and epiphyseal area (A–D) and there is a consistent decrease in their number in mutant *Gdf5-Cre;Ext1*$^{f/f}$ versus WT specimens ($p < 0.05$ by Student t-test) (E–F). By P0 (G–L), most proliferating cells in controls are present in the superficial zone (G–H) but few remain in the epiphyseal area (K–L) as a result of formation of a secondary ossification center (G–H, circled area). In P0 mutants, proliferation patterns are quite abnormal and there are fewer *H4C*-positive cells in superficial zone and more numerous positive cells scattered throughout the epiphyseal area ($p<0.05$) (I–L). *hu*, humerus. Scale bar: 350 μm for A–D and G–J.

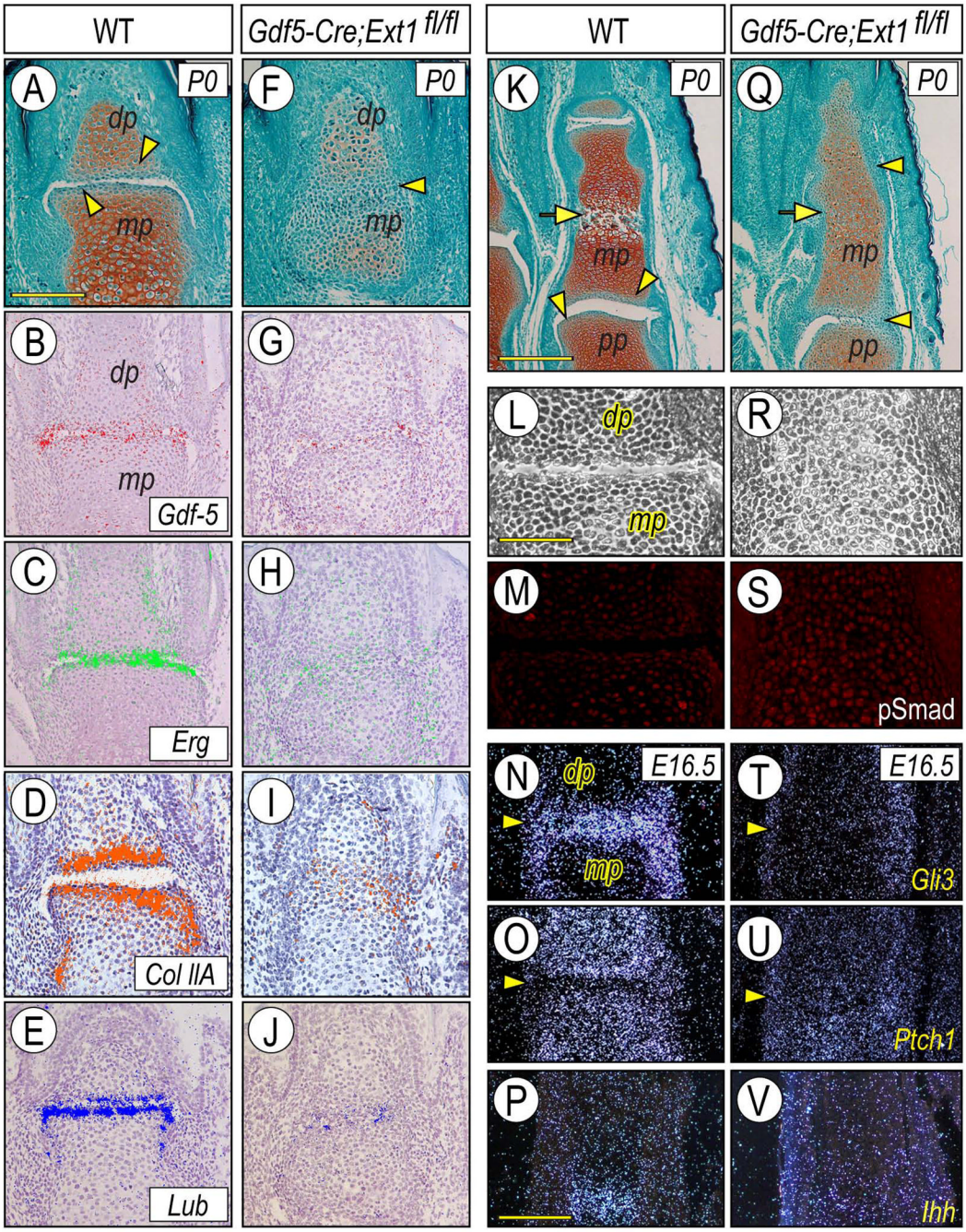

Fig. 6.

Autopod joint formation is severely affected in mutants. (A–V) Serial sections of autopods from WT and *Gdf5-Cre;Ext1*$^{f/f}$ mice were processed for Safranin-O/fast green staining, immunohistochemistry and in situ hybridization. Compared to WT littermates (A–E, K), mutant phalangeal anlagen exhibit obvious retardation of both longitudinal growth and primary ossification center formation (K, Q, arrows) and aberrant organization and even fusion of interphalangeal joints (F, Q arrowheads). Expression of *Gdf5*, *Erg*, *collagen IIA (Col IIA)* and *lubricin (Lub)* in controls is evident and restricted to joint interzone and tissues (B–E), but is negligible in severely affected mutant joints (G–J). (L–O, R–U) Compared to controls (L–P), the severely affected mutant joints contain higher levels of

immunodetectable phosphorylated Smad (pSmad) proteins (S), barely detectable *Gli3* expression in interzone (T, arrowhead) and low *Patched1* expression (U, arrowhead). Note that: in controls *Patched1* transcripts are prominent in epiphyseal chondrocytes but barely detectable in interzone itself (P, arrowhead) as shown previously (Albrecht et al., 2002); and Gli3 transcripts in mutants, though markedly reduced within the interzone, are clearly appreciable along the outer joint border as we previously showed in *Ihh*-null mice (Koyama et al., 2007a). (P, V) Ihh is strongly expressed in the diaphysis of control digit elements (P), but is barely appreciable in mutant elements displaying the severely affected joints (V). *dp*, distal phalange; *mp*, middle phalange; *pp*, proximal phalange; *ti*, tibia. Scale bars: 150 μm for A–J; 250 μm for K and Q; 100 μm for L–N and R–T; and 175 μm for O–P and U–V.

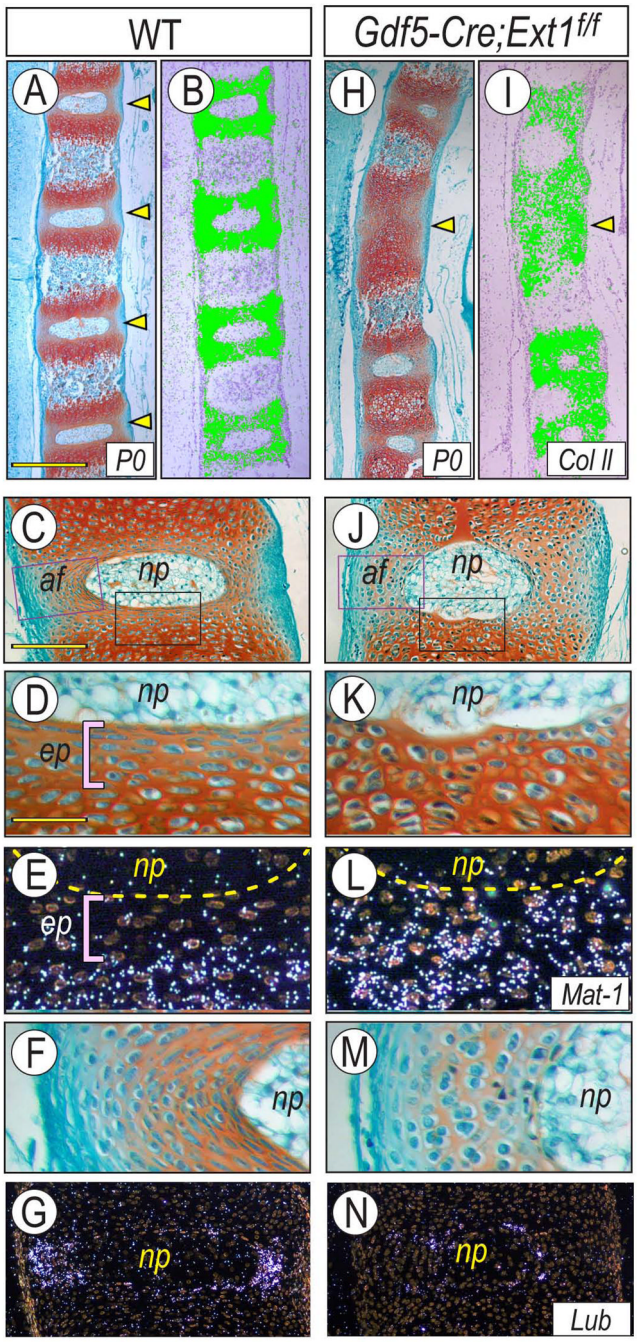

Fig. 7.

Local *Ext1* ablation deranges intervertebral disc and joint formation. (A–G) In WT P0 mice, intervertral discs (A, arrowheads) separate the Safranin-O-staining (A) and *collagen II-expressing* (B) developing vertebrae, and exhibit a typical nucleus pulposus (*np*) and a annulus fibrosus (*af*) (C) that contains flat-shaped cells (F) and expresses *lubricin* (G). The discs are flanked by endplates (*ep*) that contain flat-shaped cells also (D) and express little if any *matrilin-1* (E) and *lubricin* (G). (H–N) In P0 *Gdf5-Cre;Ext1*$^{f/f}$ littermates, the mutant discs are often missing resulting in fusion of adjacent vertebrae (H–I, arrowheads). When disc remnants are present, round-shaped cells are present in annulus (M) and endplate (K) locations, *matrillin-1* transcripts abut the nucleus pulposus (L), and *lubricin* transcripts are

virtually absent (N). Scale bars: 350 μm for A–B and H–I; 150 μm for C and G and J and N; 55 μm for D–F and K–M.

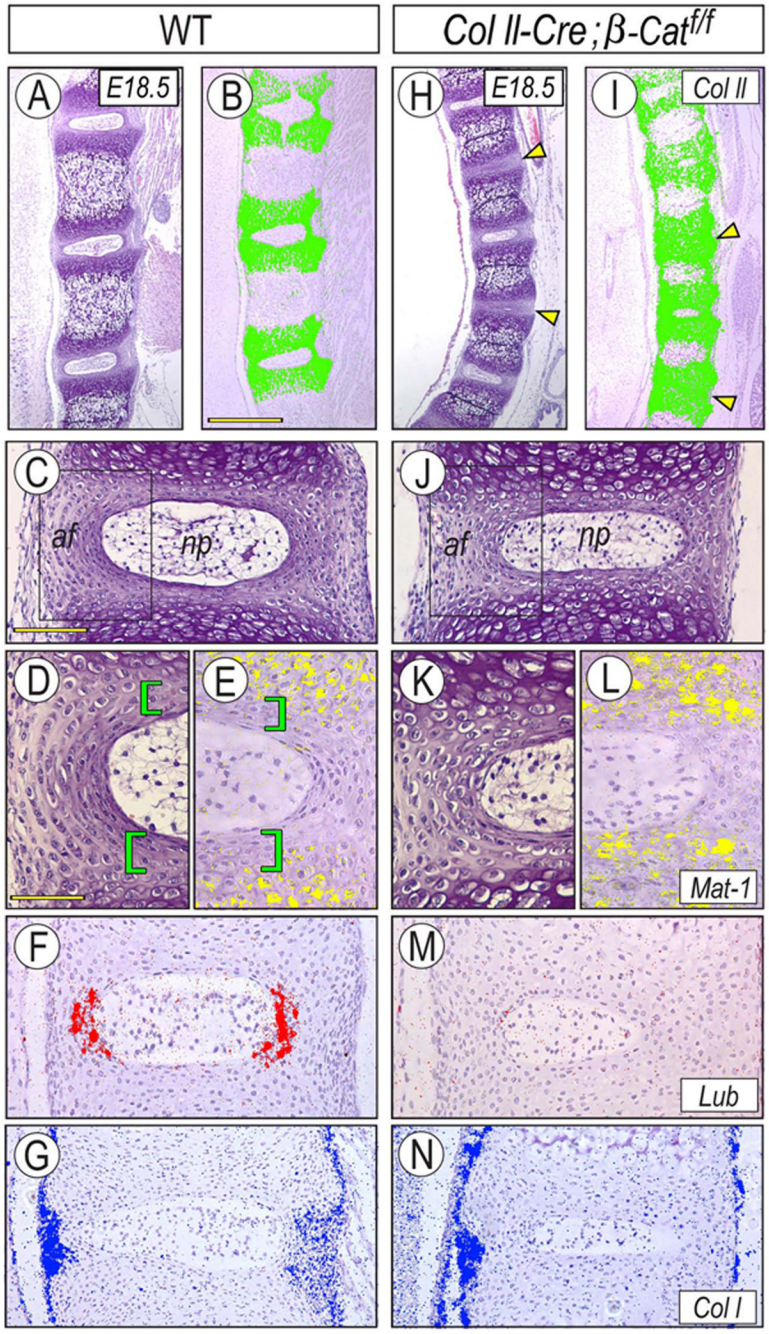

Fig. 8.

Intervertebral discs and joint formation are severely affected by conditional *β-catenin* ablation. Compared to controls (A–G), intervertebral discs and joints in *Col2a1-Cre; β-catenin*$^{f/f}$ littermates are often fused (H–I, arrowheads), and the locations of annulus fibrosus (*af*) and endplate are occupied by round-shaped cells (J–L) expressing *matrilin-1* (Mat-1) (L) but not *lubricin* (M). No *matrillin-1* expression is seen in control endplate (D–E, green brackets). (G, N) Surrounding connective tissues express *collagen I* in both WT and mutants. *af*, annulus fibrosus; *np*, nucleus pulposus. Scale bars: 350 μm for A–B and H–I; 150 μm for C, F–G, J and M–N; and 90 μm for D–E and K–L.